

# Research on productivity prediction and identification of main control factors of fractured vuggy reservoirs based on machine learning

Zhou Wang<sup>1, \*</sup>, Hongfa Liu<sup>2</sup>, Xiaolong Li<sup>3</sup>, Ligang Wang<sup>4</sup>,

Qi Yao<sup>5</sup>, Xiaolong Wang<sup>6</sup>

<sup>1</sup> Northwest Oilfield Branch, China Petrochemical Corporation, Xinjiang, China

<sup>2</sup> Northwest Oilfield Branch, China Petrochemical Corporation, Xinjiang, China

<sup>3</sup> Jiangsu Oilfield Branch, China Petrochemical Corporation, Jiangsu, China

<sup>4</sup> Northwest Oilfield Branch, China Petrochemical Corporation, Xinjiang, China

<sup>5</sup> Jiangsu Oilfield Branch, China Petrochemical Corporation, Jiangsu, China

<sup>6</sup> Northwest Oilfield Branch, China Petrochemical Corporation, Xinjiang, China

\* Corresponding Author Email: 834511240@qq.com

845826312@qq.com

1054512307@qq.com

1306535975@qq.com

992157753@qq.com

862002974@qq.com

**Abstract.** For SHB oil and gas reservoir, natural fracture development using support vector machine (SVM) and support vector regression method to SHB oil and gas field with the main fault zone of 18 flowing Wells for the single well production forecast, drilling and well completion by input data, production data and dynamic data, bottom hole flowing pressure, adjoining well production data as the input variables such as time, The predicted output value is used as the output variable for yield prediction. The results show that SVM is not only more efficient than the traditional DCA method, but also avoids geological modeling and a large amount of historical fitting work. It has a certain reference value for the formulation of rational production system in SHB block.

**Keywords:** Production forecast, Support Vector Machines, Intelligent oil production, Machine learning, Big data application.

## 1. Introduction

The dynamic prediction of oil well production has important guiding significance for understanding the reservoir, improving the working system of oil wells, and preparing scientific and reasonable development adjustment plans[1]. In the field, oil and gas reservoir numerical simulation is the most commonly used production prediction method, but it requires a lot of early geological modeling work and high-precision historical fitting. Although such a method can more accurately predict the production, geological modeling requires a lot of geological data, well structure data, fluid physical parameters; The workload of history fitting is more than that of geological modeling. In recent years, domestic and foreign scholars began to try to establish production prediction methods of oil and gas wells using machine learning or artificial neural network methods. This method can realize rapid prediction of production only through on-site production data, completion and fracturing data[2-4].

At present, many scholars have established production prediction models by using BP neural network algorithm[5-8], and some scholars have used machine learning related algorithms to predict

oil and gas well production[9-10],among which random forest algorithm and support vector machine are the most popular choices at present. From the fitting results, the method of fast prediction of oil and gas well production with the help of the related algorithm of data mining idea has a good application value.

As we all know, the production of oil and gas wells is affected by many factors, such as formation energy, wax removal cycle, oil production rate, degassing, production pressure difference, performance of adjacent wells, effectiveness of stimulation measures, changes in physical properties of crude oil, etc. For SHB fractured vuggy reservoir, since it has been put into production, most wells are still in the flowing stage, and the factors affecting its production decline also include the nature of fault zone formed due to the particularity of geological structure, The formation communication is different due to different reservoirs encountered during well drilling, and the formation pressure drop leads to new fracture cavity unit communication phenomenon. It is also difficult to define the degree of influence between various influencing factors.

At this time, the traditional production prediction method of geological modeling is not only limited by the problem that the calculation time is too long due to the excessive degree of geological heterogeneity, and the communication of new fracture cavity unit leads to the failure of single well model. Therefore, it is necessary to consider the use of data mining related algorithms for production prediction. Support vector machine (SVM) regression and support vector regression (SVR) are machine learning methods first proposed by Vapnik in 1995 on the basis of statistical theory [11]. SVM realizes nonlinear mapping to high-dimensional space through kernel function, so it is very suitable for oil well production prediction, a regression problem affected by multiple nonlinear factors. Compared with a large number of data sets required by BP neural network, the data set required by SVM is relatively small. Of course, the fitting effect is worse than that of BP neural network to a certain extent. However, given the limitation of SHB oilfield development time, well number and production data sample number, BP neural network is prone to fall into local extreme value in nonlinear prediction, affecting prediction accuracy, Instead, SVM can better solve the "small sample problem" of production prediction of SHB Oilfield Zone 1 than BP neural network.

## 2. Output prediction method based on support vector machine SVM

The support vector machine regression algorithm is a support vector machine[12] for trend prediction. Its basic principle is to map the data set in the sample to a high-dimensional space, and find a hyperplane partition space in the space, so as to classify different types of sample data. In geometry, a hyperplane is a subspace of a space, which is one dimension smaller than its space. If the data space itself is three-dimensional, its hyperplane is two-dimensional; if the data space itself is two-dimensional, its hyperplane is one-dimensional straight line. In the second classification problem, if a hyperplane can divide data into two sets, each of which contains a separate category, the hyperplane is called the "decision boundary" of data. Taking a two-dimensional plane as an example, suppose that there are several data samples in the X-Y coordinate axis, as shown in Fig.1.

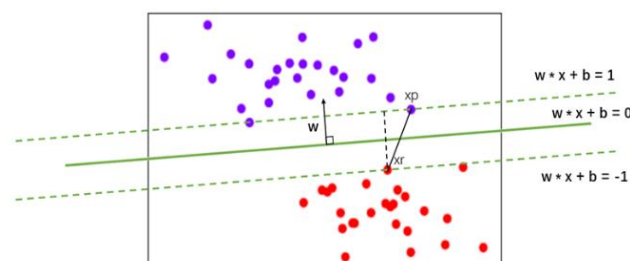


**Figure 1.** Sample SVM

Assume that the purple point label is 1, the red point label is - 1, and the hyperplane of two-dimensional data is a one-dimensional line. Use the hyperplane to divide the purple and red points.

Assume that this line is  $\omega \cdot x_p + b = 0$ . When the linear translation reaches the first purple point, there are:

$$\omega \cdot x_p + b = p \quad (1)$$

When the linear translation reaches the first red point, there are:

$$\omega \cdot x_r + b = r \quad (2)$$

In order to find the maximum intercept d, since p and r should be symmetrical in numerical value, divide both sides of equation 1 and equation 2 by p at the same time to get the following formula:

$$\omega \cdot x_p + b = 1 \quad (3)$$

$$\omega \cdot x_r + b = -1 \quad (4)$$

Subtract the two equations to get:

$$\omega \cdot (x_p - x_r) + b = 2 \quad (5)$$

$$d = \frac{2}{\|\omega\|} \quad (6)$$

To find the maximum d, find minimum value of  $\omega$ , elimination seeking  $\omega$  the possible root sign caused by the module length of, therefore  $\omega$  the module length is squared to obtain:

$$\min_{\omega, b} \frac{\|\omega\|^2}{2} \quad (7)$$

$$y_i [\omega \cdot x_i + b] - 1 \geq 0, \quad i = 1, 2, \dots, l, \quad (8)$$

This is the optimal classification plane[13] mentioned in many literatures, that is, loss function.

For the solution of the optimal classification plane in any dimensional space  $\omega$  is zero, otherwise the hyperplane will be directly reduced by two or more dimensions, resulting in  $b=0$  in the above functions, and the following conditions cannot be met:

$$y_i [\omega \cdot x_i + b] - 1 \geq 0, \quad i = 1, 2, \dots, l, \quad (9)$$

To avoid this situation, when the loss function is a quadratic function and the constraint condition is a linear constraint condition, the optimization problem becomes a convex optimization problem, which can be solved by using the Lagrange multiplier method, namely:

$$L(\omega, b, \alpha) = \frac{1}{2} \|\omega\|^2 - \sum_{i=1}^N \alpha_i (y_i (\omega \cdot x_i + b) - 1) (\alpha_i \geq 0) \quad (10)$$

Let the dual problem of function X be solved, and the dual problem can also be obtained at the same time of finding  $\omega$ , and the optimal solution of dual function can be obtained by using.

$$\Delta = \min_x L(x, \alpha) - \max_{\alpha} g(\alpha) \quad (11)$$

When  $\Delta = 0$ , the strong dual problem is used instead of solving the optimal solution of the original function. After satisfying Karush Kuhn Tucher (KKT) condition, we get:

$$\min_{\omega, b} \max_{\alpha_i \geq 0} L(\omega, b, \alpha) = \max_{\alpha_i \geq 0} \min_{\omega, b} L(\omega, b, \alpha) \quad (12)$$

Therefore, the maximum value of the dual problem can be solved  $\alpha$ , that is, find the maximum value of the function:

$$\max_{\alpha_i \geq 0} \left( \sum_{i=1}^N \alpha_i - \frac{1}{2} \sum_{i,j=1}^N \alpha_i \alpha_j y_i y_j x_i \cdot x_j \right) \quad (13)$$

For nonlinear problems, the data needs to be mapped from the independent variable  $x$  of the original space to the new space. At this time, the loss function of nonlinear SVM can be obtained by analogy with the loss function of linear SVM:

$$\min_{\omega, b} \frac{\|\omega\|^2}{2} \quad (14)$$

Subject to:  $y_i(\omega \cdot \Phi(x_i) + b) \geq 1$

$$i = 1, 2, \dots, N \quad (15)$$

Its corresponding Lagrange function and Lagrange dual function:

$$L(\omega, b, \alpha) = \frac{1}{2} \|\omega\|^2 - \sum_{i=1}^N \alpha_i (y_i (\omega \cdot \Phi(x_i) + b) - 1) \quad (16)$$

$$L_d = \sum_{i=1}^N \alpha_i - \frac{1}{2} \sum_{i,j} \alpha_i \alpha_j y_i y_j \Phi(x_i) \cdot \Phi(x_j) \quad (17)$$

Then use the gradient descent pair  $\alpha$  Finally, the decision boundary function is obtained as follows:

$$f(x_{\text{test}}) = \text{sign}(\omega \cdot \Phi(x_{\text{test}}) + b) = \text{sign} \left( \sum_{i=1}^N \alpha_i y_i \Phi(x_i) \cdot \Phi(x_{\text{test}}) + b \right) \quad (18)$$

In order to solve the problem of dimension increase and exponential increase of calculation amount caused by , the "kernel technique" is introduced to map the vector in the original space  $x$  to in the form of dot product. Substitute for , that is:

$$K(\mu, \nu) = \Phi(\mu) \cdot \Phi(\nu) \quad (19)$$

This formula is called the kernel function. Combined with the fact that the kernel function in SVM is a positive definite kernel function and satisfies Mercer's law, it can ensure that the high-dimensional space can be represented by the dot product of two vectors in the low dimensional space.

Different kernel functions are selected to solve the hyperplane search problem under different data distributions. The four common kernel functions of SVM are shown in Table 1:

**Table 1.** Four Kernel Functions Commonly Used in SVM

Input	Meaning	Solve the problem	Kernel function expression
“linear”	Linear kernel	Linear	$K(x, y) = x^T y = x \cdot y$
“poly”	Polynomial kernel	Partial linearity	$K(x, y) = (\gamma(x \cdot y) + r)^d$
“sigmoid”	Hyperbolic tangent kernel	Nonlinear	$K(x, y) = \tanh(\gamma(x \cdot y) + r)$
“rbf”	Gaussian radial basis	Partial nonlinearity	$K(x, y) = e^{-\gamma \ x - y\ ^2}, \gamma > 0$

In order to deal with incompletely linearly separable data sets, it does not mean that we can get better results by narrowing the margin of "hard interval". If two groups of data can be almost linearly separable within a certain error tolerance, that is, there are a few points that are wrongly classified within the original hard interval margin. At this time, because the error cannot be eliminated, the error remains zero as before, and the original hard interval will be converted into "soft interval".

In the soft interval, the decision boundary can tolerate a small part of the training error, that is, SVM attempts to find the balance between the maximum margin and the number of samples of the wrong class. Therefore, a new loss function is defined:

$$\min_{\omega, b, \zeta} \frac{\|\omega\|^2}{2} + C \sum_{i=1}^n \zeta_i \quad (20)$$

Subject to:  $y_i(\omega \cdot \Phi(x_i) + b) \geq 1 - \zeta_i$

$$\zeta_i \geq 0 \quad (21)$$

$$i = 1, 2, \dots, N \quad (22)$$

Where, C is the coefficient used to control the penalty term, and  $\zeta_i$  is the relaxation coefficient, that is, the mathematical expression of the number of samples allowed to be wrongly classified. At this time, the Lagrange function becomes:

$$L(\omega, b, \alpha, \zeta) = \frac{1}{2} \|\omega\|^2 + C \sum_{i=1}^N \zeta_i - \sum_{i=1}^N \alpha_i (y_i (\omega \cdot \Phi(x_i) + b) - 1 + \zeta_i) - \sum_{i=1}^N \mu_i \zeta_i \quad (23)$$

The KKT conditions to be met are:

$$\frac{\partial L(\omega, b, \alpha, \zeta)}{\partial \omega} = \frac{\partial L(\omega, b, \alpha, \zeta)}{\partial b} = \frac{\partial L(\omega, b, \alpha, \zeta)}{\partial \zeta} = 0 \quad (24)$$

$$\zeta_i \geq 0, \alpha_i \geq 0, \mu_i \geq 0 \quad (25)$$

$$\alpha_i (y_i (\omega \cdot \Phi(x_i) + b) - 1 + \zeta_i) = 0 \quad (26)$$

$$\mu_i \zeta_i = 0 \quad (27)$$

Lagrange dual function:

$$L_D = \sum_{i=1}^N \alpha_i - \frac{1}{2} \sum_{i,j} \alpha_i \alpha_j y_i y_j \Phi(x_i) \Phi(x_j) \quad (28)$$

Subject to  $C \geq \alpha_i \geq 0$

It is worth noting that after the introduction of soft interval, the Lagrange multiplier  $\alpha$  From original  $\alpha \geq 0$  becomes  $0 \leq \alpha \leq C$ , otherwise the function will have no solution.

### 3. Application examples

#### 3.1. Overview of SHB Oil and Gas Fields

The burial depth of the SHB oil and gas field zone is generally more than 7000m, which belongs to the reservoir controlled by fracture cavity fault solution of ultra deep carbonate rocks. At present, most wells are still in the elastic drive stage. Due to the control of natural fractures in the reservoir, it is easy to reach the boundary control flow regime, and the fracture cave unit contains less water (<1%). At present, there are 18 wells in No. 1 main fracture zone, with the maximum controlled reserves of 15.58742 million tons. The physical property of the oil is good, belonging to low waxy light crude oil. The reservoir has good mobility, and the equivalent permeability is up to 1980mD. First, try to use the traditional Arps decline curve to fit the historical production data, and the fitting effect of some wells is shown in Fig.2.

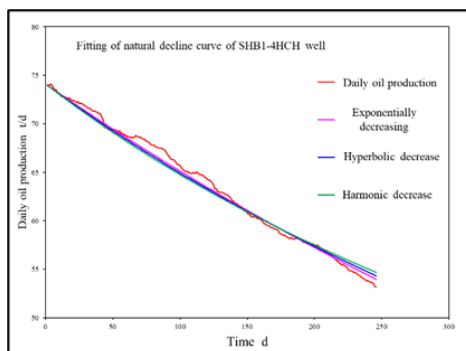


**Figure 2.** Natural decline curve fitting of SHB1-4HCH well

The purpose of traditional Arps decline fitting in stages is to compare the fitting effect with SVM, use the traditional Arps decline method to fit the production data to obtain the decline rate, and then obtain the Arps production forecast chart for the next five months. By comparing the actual production data of wells after May 5, 2020, as shown in Fig.3.

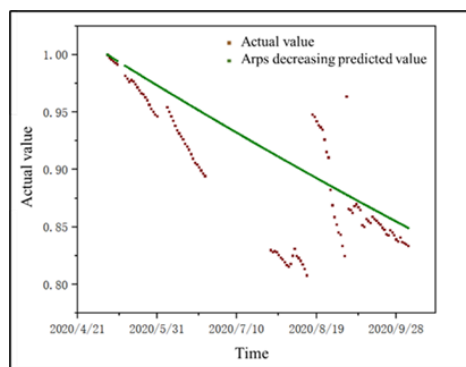


**Figure 3.** Comparison between Arps decline prediction value and actual value

It can be seen from the yield fitting curve and the yield prediction comparison curve that even under the high fitting degree, the traditional Arps decline curve analysis method (DCA) still has a large error in long-term prediction.

### 3.2. Data selection and preprocessing

There are many factors that affect the accuracy of production prediction, such as natural energy of reservoir, nature of fault zone, wax removal cycle, oil production rate, degassing, production pressure difference, adjacent well performance, changes in crude oil physical properties, etc. These influencing factors affect each other. For example, the natural energy of the reservoir, i.e. the residual pressure in the middle, must affect whether degassing occurs or not and the degassing radius, while the nature of the fault zone directly affects the abundance of natural energy and the speed of oil production.

Therefore, drilling and completion data, production performance data, bottom hole flowing pressure data, production time of adjacent wells and other data are selected as input variables, and production prediction value is used as output variable for production prediction.

The first thing to be solved is how to obtain continuous bottom hole flowing pressure data. Because SHB Oilfield belongs to fracture vug reservoir, it is reasonable to calculate the bottom hole flowing pressure of SHB block by referring to the bottom hole flowing pressure algorithm of Du Xin[14] et al., and other methods include the beggs-brill method and the multi segment method[15]. The continuous bottom hole flowing pressure of each well can be calculated by comparing and selecting the four segment method, Then, by comparing with the data measured by the pressure gauge, the relationship between bottom hole flowing pressure and production time is obtained as shown in the figure:

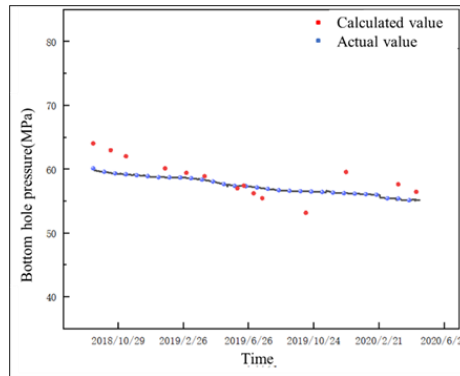


**Figure 4.** Calculated and Actual Bottom Hole Flow Pressure of Well SHB1-1H

It can be seen from the figure that the calculated bottom hole flowing pressure is slightly lower than the measured bottom hole flowing pressure, and the error is basically about 5.7%. It can also be seen from the change of bottom hole flow pressure with time that the traditional Arps and modern Fetkovich decline analysis methods can not be used in SHB fracture cavity reservoirs fundamentally, because both of them require the bottom hole flow pressure to be basically stable [16-18].

Because the production performance data, bottom hole flowing pressure data, drilling and completion data and relevant data units are inconsistent, it needs to be normalized in advance and cleaned in advance. The role of normalization is unique to SVM and must be carried out. In order to integrate the data that are interrelated but difficult to define the degree of correlation, SVM can only train the data set through data normalization processing without giving data association. The specific normalization method is as follows:

$$x_s = (x - x_{\min}) / (x_{\max} - x_{\min}) \quad (29)$$

Where,  $x$  represents the normalized variable,  $x_{\min}$  represents the minimum value of the parameter in the dataset, and  $x_{\max}$  represents the maximum value of the parameter in the dataset.

The main task of data cleaning is to clean the abnormal data in the data set, such as production mutation caused by short-term nozzle adjustment, data loss caused by shut in and pressure build-up process, and unstable production at the initial stage of production.

In order to reflect the impact of production of adjacent wells on the production performance of old wells, the production time of 18 wells is also taken as a link in the input variable  $x$ . As the injection production well system of the whole block is still in the process of gradual improvement, taking this factor into account can also predict the future short-term (generally within one year) production fluctuations caused by the production of new wells.

Since the current production dynamic data only includes the wax scraping cycle data, it is impossible to describe the specific wax deposition process. Therefore, referring to the processing method in [19-20], it is believed that the wax deposition process should be linear. Therefore, it is assumed that the wax crystal accumulation process between two wax removal time nodes is also linear, and normalized.

### 3.3. Model training and parameter adjustment

The final valid data set contains  $17302 \times 7 = 121114$  pieces of data, of which 70% are randomly selected as the data training set and 30% as the verification set. The four parameters of the model are set as follows:  $C=10$ , kernel=RBF,  $\gamma=0.8$ ,  $\epsilon=0.01$ .

The daily output of 18 single wells is predicted, but the daily output of single wells between 0-400 days is still well matched. The determination coefficients of some wells reach  $R^2=0.9995$ ,  $MES=0.001938$ , and  $MAE=0.009659$ . However, generally speaking, the 18 wells show different degrees of abnormality after the prediction exceeds 400 days. It shows that if the prediction is made for a long time, it will cause a large error. This can also be proved by fitting the error distribution diagram (Fig.7).

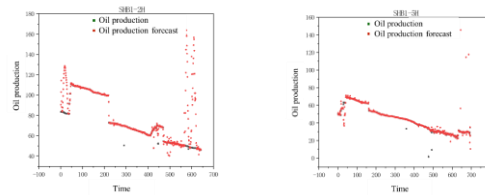


**Figure 5.** Comparison between SHB1-2H and SHB1-5H Oil Production and Predicted Oil Production

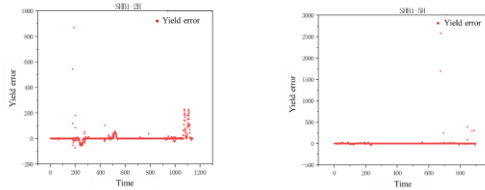


**Figure 6.** Error of SHB1-2H and SHB1-5H Predicted Oil Production

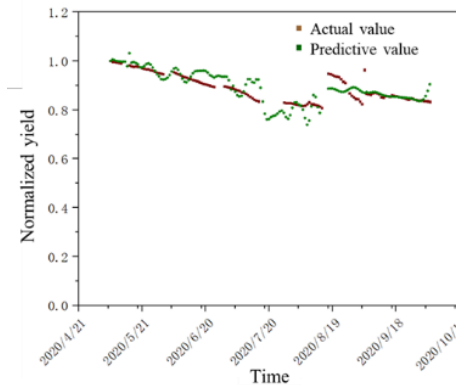


**Figure 7.** Comparison between Actual and Predicted Values of SHB1-4HCH Well after Normalized Production

Compared with Arps decline prediction chart, SVM production prediction can not only extend the prediction time, but also has a much higher prediction accuracy than Arps decline prediction. To some extent, it can also reflect the surplus elasticity. The following table shows the predictable days and average error distribution of 18 wells. The overall average error is less than 3.5%, indicating that the fitting effect is good.

**Table 2.** Predictable days and mean error distribution table

Well name	Days	Average error
SHB1-1H	924	0.89%
SHB1-2H	741	9.63%
SHB1-3	1044	0.48%
SHB1-4HCH	472	4.65%
SHB1-5H	897	8.27%
SHB1-6H	1180	1.62%
SHB1-7H	1143	1.36%
SHB1-8H	914	1.54%
SHB1-9	733	0.53%
SHB1-10H	783	3.55%
SHB1-11	488	2.01%
SHB1-12	287	2.38%
SHB1-13CH	289	2.12%
SHB1-15	496	8.47%



SHB1-17H	370	4.79%
SHB1-20H	408	1.24%
SHB1-21	115	0.82%
SHB1-24X	84	0.22%

### 3.4. Identification of main control factors affecting production decline

According to the influencing factors contained in the database, the decline influencing factors are identified from the geological and production dynamic aspects. In terms of fracture properties, the average decline rate of each fracture property is 1# pull apart<1# extrusion<1# translation<1# strike slip;5# extrusion<5# translation; The difference in natural energy caused by the difference in the size and memory of the fracture cavity body shows that the natural energy of each fault zone shows a completely opposite law to the nature of the fault, that is, 1# pull apart>1# extrusion>1# translation>1# strike slip, 5# extrusion<5# translation; Finally, we believe that the geological factors have a major impact on the decline because the pull section can provide the highest natural energy, so the decline rate is the lowest.

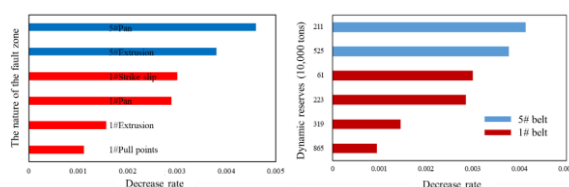


**Figure 8.** Relationship between the nature of fault zone and dynamic reserves and decline rate

In addition, wellbore degassing, wax scraping, oil production rate and adjacent well performance mainly affect decline rate of single well and well group from production means. Degassing leads to the increase of crude oil viscosity and the decline of wellbore lifting capacity; After calculation, the degassing depth 2000 increases with the increase of depth decline rate, and the degassing depth should be controlled to control the decline. Since the initial production of the well is high and the flow rate is fast, most of the wax crystals are carried out of the wellbore by the fluid, the formation energy is sufficient, and the wax removal cycle has an obvious impact on the decline rate, so the wax removal cycle should be reasonably shortened to maintain stable production.

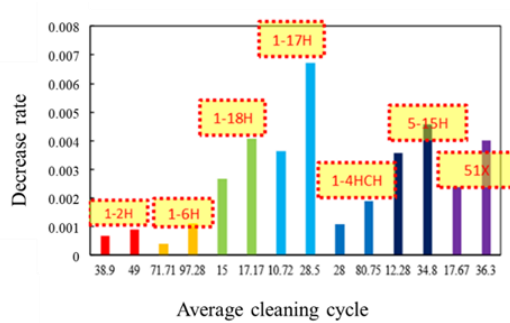


**Figure 9.** Effect of wellbore degassing and wax scraping frequency on decline rate

The influence of oil production rate on decline rate is very important. High oil production rate often means high decline rate. Controlling reasonable oil production rate will help to expand the well bore coverage, communicate with new reservoirs and control decline. In the process of continuously improving the layout of production wells in the block, the overall production of the well cluster increases, but at the same time, it also leads to accelerated loss of formation energy. In terms of decline rate, the decline rate rises rapidly. It is necessary to reasonably allocate production to control the comprehensive recovery rate of the well cluster, monitor the dynamic impact of adjacent wells, and select a reasonable time for water injection in the well cluster to delay the decline of the well cluster.

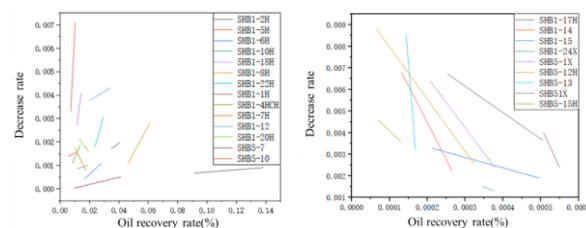


**Figure 10.** Declining rate under communication without new reserves (left);Declining rate under communication with new reserves (right)

### 3.5. Decreasing influence factor weight

Through SVM and SVR decline influence weight identification, before wellbore degassing, the weight ranking of oil production rate > bottom hole flowing pressure > temporary well performance > fracture property > back pressure > wax accumulation thickness > degassing is often displayed; After wellbore degassing, the influence weight ranking of production rate (weight reduction) > bottom hole flowing pressure (weight increase) > near well performance > fracture property > degassing > wax thickness > back pressure is shown; After formation degassing, the weight of oil production rate further decreases, but it still shows the weight ranking of oil production rate>bottom hole flowing pressure (weight reduction) > degassing > fracture property > wax accumulation thickness > back pressure > near well performance.

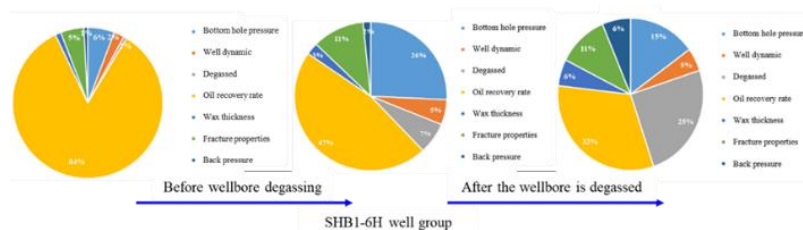


**Figure 11.** Ranking of Factors Affecting Decline Rate in Different Production Stages of Well Cluster SHB1-6H

Under the premise of the above weight laws, the influencing factors of typical well groups SHB1-6H, SHB1-14, SHBP3H, 5# north section and 5# south section are slightly different due to the difference of current formation pressure and oil production rate. Among them, SHB1-6H well group shows typical weight ranking of oil production rate>bottom hole flowing pressure>temporary well performance>degassing>fracture property>wax thickness>back pressure; However, SHB1-14 well group has a higher influence on fracture properties due to the insufficient fracture energy compared with SHB1-6H well group, which shows the weight ranking of oil production rate>fracture properties>bottom hole flow pressure>degassing>near well performance>back pressure>wax deposition thickness; Due to the serious degassing phenomenon,SHBP3H well group shows the weight ranking of oil production rate>degassing>bottomhole flowing pressure>temporary well performance>fracture property>wax accumulation thickness>back pressure; Although the geological reserves of the 5# fault zone are larger than that of the 1# fault zone, most of the faults are strike slip unfavorable, and the communication effect between wells is poor. Therefore, the 5# fault zone shows the weight ranking of oil production rate>bottom hole flow pressure>fracture property>wax deposition thickness>degassing>back pressure>near well performance. However, it conforms to the overall weight ranking of SHB.

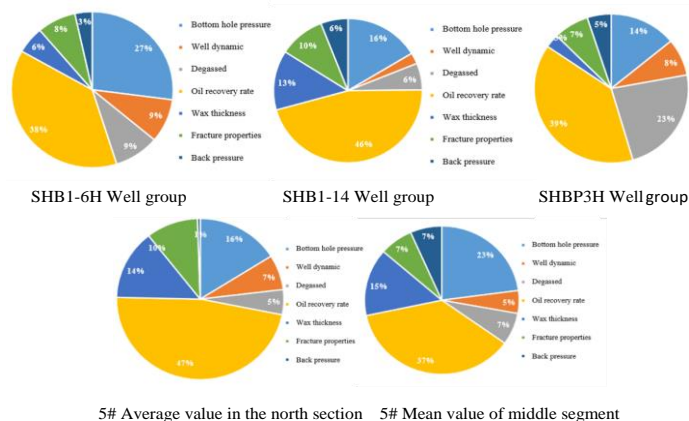


**Figure 12.** Ranking of factors affecting decline rate of typical well groups

## 4. Conclusions and suggestions

1) By using the methods of support vector machine (SVM) and support vector regression (SVR), the production prediction of 18 wells in the main fault zone of Zone 1 in Zone 1 was completed by inputting production performance data, drilling and completion data, bottom hole flowing pressure data, production time and other data of production wells in the block.

2) Compared the traditional Arps decline prediction output with the prediction output based on SVM, although the traditional Arps has a very high fitting effect on the historical production data, it is not only unable to achieve the medium and long-term output prediction in the aspect of output prediction, but also the output prediction effect is worse than that of SVM.

3) With a high coefficient of determination, the accuracy of SVM for the prediction of more than 400 days is still questionable. However, for the production prediction of less than 400 days, including the comparison with the actual production from May 5 to October 5, there is a small prediction error, and the average prediction error is only 3.03%. It shows that this method can still have high prediction accuracy when the data sample is small, and does not need geological modeling, which can be further applied to the production optimization research of reservoir development.

4) Referring to the current DCA curve of low pressure wells, when the formation energy weakens to a certain extent, the wax scraping cycle will become shorter, and the daily output of a single well will fluctuate similar to that of the prediction chart. Analogically, the error increase of SVM daily production prediction over 400 days may be caused by the reduction of formation energy and the increase of wax scraping and other measures on the production prediction. This will be the focus of the next step.

5) The prediction curve of daily production of single well can also reflect the remaining elastic recoverable reserves to a certain extent. However, since this chart is only predicted at a certain nozzle, i.e. a fixed recovery rate, and no variable oil production rate prediction is made, it is still impossible to determine the specific elastic recoverable reserves, nor the impact of oil production rate on elastic recoverable reserves.

## 5. References

- [1] LIU Wei, LIU Wei, GU Jianwei. Prediction of daily oil production of oil wells based on machine learning method[J]. Petroleum drilling and production technology, 2020, 42(01): 70-75.
- [2] ZHANG Haoran. Analysis Method of Oilfield Production Performance Based on BP Neural Network[J]. Petrochemical technology, 2015, 22(06): 124.
- [3] Liu, Wei, et al. "Predictive model for water absorption in sublayers using a machine learning method." Journal of Petroleum Science and Engineering 182 (2019): 106367.

- [4] GU Jianwei, ZHOU Mei, LI Zhitao, JIA Xiangjun, LIANG Ying. Prediction Method of Oil Well Production Based on Long term and Short term Memory Network Model of Data Mining[J]. Special oil and gas reservoir, 2019, 26(02): 77-81+131.
- [5] LI Yanzun, BAI Yuhu, CHEN Guihua, XU Binxiang, CHEN Ling, DONG Zhiqiang. New technology for shale oil and gas production prediction based on artificial neural network method——Take Eagle Ford Shale Oil and Gas Field in the United States as an example[J]. China Offshore Oil and Gas, 2020, 32(04): 104-110.
- [6] LI Juhua, CHEN Chen, XIAO Jialin. Production prediction of shale gas multi-stage fracturing wells based on stochastic forest algorithm[J]. Journal of Changjiang University (Natural Science Edition), 2020, 17(04): 34-38+7.
- [7] REN Yanlong, GU Jianwei, CUI Wenfu, ZHANG Yigen. Prediction model of oilfield production based on improved drosophila algorithm and short-term memory neural network[J]. Science, technology and engineering, 2020, 20(18): 7245-7251.
- [8] Kiss, Akos, et al. "Formation breakdown pressure prediction with artificial neural networks." SPE International Hydraulic Fracturing Technology Conference and Exhibition. Society of Petroleum Engineers, 2018.
- [9] ZHU Qingzhong, HU Qiuja, DU Haiwei, FAN Bin, ZHU Jie, ZHANG Bin, ZHAO Yuhua, LIU Bin, TANG Jun. Model of coalbed methane vertical well gas production based on stochastic forest algorithm[J]. Journal of Coal Industry, 2020, 45(08): 2846-2855.
- [10] Fulford, David S., et al. "Machine learning as a reliable technology for evaluating time/rate performance of unconventional wells." SPE Economics & Management 8.01 (2016): 23-39.
- [11] Sain, Stephan R. "The nature of statistical learning theory." (1996): 409-409.
- [12] Zhang, Lining, Lipo Wang, and Weisi Lin. "Semisupervised biased maximum margin analysis for interactive image retrieval." IEEE Transactions on Image Processing 21.4 (2011): 2294-2308.
- [13] GAO Xinyi, HAN Fei. Grain yield prediction based on support vector machine with hybrid intelligent algorithm[J]. Journal of Jiangsu University (Natural Science Edition), 2020, 41(03): 301-306.
- [14] DU Xin, LU Zhiwei, LI Dongmei, XU Yandong, LI Peichao, LU Detang. Analysis of the Bottom Hole Pressure of the Coupled Model of the Fluctuation and Flow in Fractured Cavity Reservoirs[J]. Applied Mathematics and Mechanics, 2019, 40(04): 355-374.
- [15] Sinha, M.K. and L.R. Padgett, Static/Flowing Bottomhole Pressure for A Gas Well, in Reservoir Engineering Techniques Using Fortran, M.K. Sinha and L.R. Padgett, M.K. Sinha and L.R. Padgett^Editors. 1985, Springer Netherlands: Dordrecht. p. 183-190.
- [16] XIAO Cui. Application of Modern Production Decline Analysis Method in South Yanchuan Coal Seam Gas Field in Ordos Basin[J]. Natural gas industry, 2018, 38(S1): 102-106.
- [17] Sureshjani M H , Gerami S . A New Model for Modern Production-Decline Analysis of Gas/Condensate Reservoirs[J]. Journal of Canadian Petroleum Technology, 2011, 50(7-8):p.10-23.
- [18] Bahadori A . Analysing gas well production data using a simplified decline curve analysis method[J]. Chemical Engineering Research & Design, 2012, 90(4):541-547.
- [19] ZHONG Jieyun, DU Hongyan. Analysis of the Factors Related to Wax Deposition in Oil Wells and Wax Control Measures[J]. Chemical management, 2013(14): 139.
- [20] YANG Fan. Refine the wax removal and control system of oil wells to ensure stable production of oil wells[J]. Chemical Design Communication, 2017(4).